Chemosphere 286 (2022) 131596

Contents lists available at ScienceDirect

Chemosphere

journal homepage: www.elsevier.com/locate/chemosphere

Why is calcite a strong phosphorus sink in freshwater? Investigating the adsorption mechanism using batch experiments and surface complexation modeling

Hilary Flower [a,b,*], Mark Rains [b], Yasemin Taşcı [b,1], Jia-Zhong Zhang [c], Kenneth Trout [b], David Lewis [d], Arundhati Das [b,e], Robert Dalton [b]

[a] Eckerd College, 4200 54th Ave S, St. Petersburg, FL, 33711, United States
[b] School of Geosciences, University of South Florida, 4202 E. Fowler Ave, Tampa, FL, 33620, United States
[c] Ocean Chemistry and Ecosystems Division, Atlantic Oceanographic and Meteorological Laboratory, National Oceanic and Atmospheric Administration, Miami, FL, 33149, United States
[d] Department of Integrative Biology, University of South Florida, 4202 E. Fowler Ave, Tampa, FL, 33620, United States
[e] Chemical Engineering, University of South Florida, 4202 E. Fowler Ave, Tampa, FL, 33620, United States

HIGHLIGHTS

- A model of phosphorus adsorption to calcite in natural waters is presented.
- Immersion in freshwater enhances phosphorus adsorption to the calcite mineral surface.
- Phosphorus preferentially adsorbs to calcite as $CaPO_4^-$ in freshwater.
- Abundance of dissolved $CaPO_4^-$ in freshwater enhances phosphorus adsorption.
- Phosphorus competes with CO_3^{2-} at the calcite surface more effectively in freshwater compared to seawater.

GRAPHICAL ABSTRACT

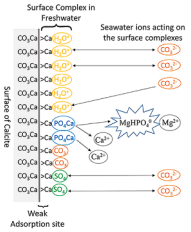

ARTICLE INFO

Handling Editor: X. Cao

Keywords:
Calcium carbonate
Phosphates
Abiotic factors
Sediment dynamics
Nutrient

ABSTRACT

One of the primary drivers of Phosphorus (P) limitation in aquatic systems is P adsorption to sediments. Sediments adsorb more P in freshwater compared to other natural solutions, but the mechanism driving this difference is poorly understood. To provide insights into the mechanism, we conducted batch experiments of P adsorption to calcite in freshwater and seawater, and used computer software to develop complexation models. Our simulations revealed three main reasons that, combining together, may explain the greater P adsorption to calcite in freshwater vs. seawater. First, aqueous speciation of P makes a difference. The ion pair $CaPO_4^-$ is much more abundant in freshwater; although seawater has more Ca^{2+} ions, $MgHPO_4^0$ and $NaHPO_4^0$ are more thermodynamically favored. Second, the adsorbing species of P make a difference. The ion pair $CaPO_4^-$ (the preferred adsorbate in freshwater) is able to access adsorption sites that are not available to HPO_4^{2-} (the preferred adsorbate in seawater), thereby raising the maximum concentration of P that can adsorb to the calcite surface in freshwater. Third, water chemistry affects the competition among ions for surface sites. Other ions (including P)

* Corresponding author. Eckerd College, 4200 54th Ave S, St. Petersburg, FL, 33711, United States.
E-mail address: flowerhd@eckerd.edu (H. Flower).
[1] Current address for Yasemin Taşcı: Tarım ve Orman Bakanlığı, Su Yönetimi Genel Müdürlüğü, Beştepe Alparslan Türkeş Cad, Cumhurbaşkanlığı Blv No:71, 06510 Yenimahalle/Ankara - Turkey.

https://doi.org/10.1016/j.chemosphere.2021.131596
Received 21 May 2021; Received in revised form 13 July 2021; Accepted 16 July 2021
Available online 21 July 2021

compete more effectively against CO_3^{2-} when immersed in freshwater vs. seawater, even when the concentration of HCO_3^-/CO_3^{2-} is higher in freshwater vs. seawater. In addition, we found that under oligotrophic conditions, P adsorption is driven by the higher energy adsorption sites, and by the lower energy sites in eutrophic conditions. This study is the first to model P adsorption mechanisms to calcite in freshwater and seawater.

1. Introduction

Inorganic phosphorus (P) is an essential nutrient in terrestrial and estuarine ecosystems. Any change in P availability is important in aquatic ecosystems because it regulates primary productivity, and if it is in excess it can lead to eutrophication. In a recent global meta-analysis, P limitation of aboveground plant production was much more pervasive than previously thought, comprising nearly half of the 652 natural terrestrial ecosystems studied (Hou et al., 2020). Because of the sensitivity of terrestrial and coastal ecosystems to P availability, it is important to understand the processes that regulate P fluxes.

Dissolved P enters aquatic systems naturally due to dissolution of phosphate minerals such as apatite, and as a result of human impacts such as soil erosion, deforestation, sewage injection, and the use of fertilizers (Riemersma et al., 2006). Because dissolved P adsorbs strongly to sediment and soil when immersed in freshwater, this depresses dissolved P concentrations in favor of higher particulate P concentrations (Bowes, 2003; Owens and Walling, 2002). Consequently, adsorption drives P limitation in many terrestrial ecosystems, a process termed "sink-driven P limitation" (Paludan and Morris, 1999; Vitousek et al., 2010). In many freshwater ecosystems, P adsorption to soil reduces eutrophication downstream, and for this reason wetland soil has been harnessed for mitigation purposes (Reddy and Graetz, 1981; Richardson, 1985; Vitousek et al., 2010).

Strong P adsorption to sediments appears to be a feature of immersion in freshwater, as the same is not observed for immersion in seawater (Zhang and Huang, 2011). Because P adsorption is a major driver of P fluxes in freshwater environments, it is important that we understand the mechanism governing it. Unfortunately, we have not as yet established quantitatively the exact chemical reactions that cause P to adsorb to sediment so strongly in freshwater. Understanding these chemical reaction mechanisms would allow us to better predict P availability in both freshwater regions. Filling this knowledge gap becomes more urgent in the face of increasing human perturbation on the P cycle in aquatic environments (Prastka et al., 1998; Filippelli, 2008). Accordingly, the present study aims to answer the question: Why does P adsorb more strongly to calcite when immersed in freshwater vs. seawater?

Previous laboratory experiments can provide valuable clues. In simple CaCO3 and NaCl solutions, the presence of both Ca^{2+} and Mg^{2+} enhances P adsorption, making cooperative adsorption of Ca^{2+}-P and Mg^{2+}-P pairs at the surface of $CaCO_3$ and goethite seem likely (Millero et al., 2001; Gao and Mucci, 2003). However, laboratory experiments cannot test the plausibility of specific alternative chemical reactions, nor test for the effects of single ions in complex electrolyte solutions such as natural freshwater. Geochemical modeling is a tool that uses chemical thermodynamics to investigate plausible chemical reactions to explain field observations. Researchers studying a wide range of adsorbates and adsorbents have used computer programs to develop surface complexation models to explain the adsorption behavior observed in the laboratory and field (Dzombak and Morel, 1990).

To investigate, it was necessary to choose a mineral phase, because the precise chemical reactions of P at the mineral surface depends on the composition of the solid particle. We chose to focus on calcite as the adsorbing surface in the present study because adsorption of P to $CaCO_3$ minerals is thought to be a major control of P concentrations in freshwater settings (Riemersma et al., 2006) and marine settings (de Kanel and Morse, 1978; Morse et al., 1985). Further, many coastal regions are carbonate-based, such as northeast Qatar on the Persian Gulf, the Ryukyus of Japan, the Maltese Islands, Mallorca, Spain, and the Florida Everglades (Shinn, 1973; Zhou and Li, 2001; Kogure et al., 2006; Brandano et al., 2009; Garing et al., 2013). Calcite is the dominant form of calcium carbonate at the Earth's surface (Lee et al., 2016). Yet few studies have considered how the interaction of calcite and seawater affects P adsorption dynamics.

An additional advantage in focusing on calcite is that surface complexation reactions and affinity constants for $CaHPO_4^0$, $CaPO_4^-$, and HPO_4^{2-} are available in the literature to be used as a launchpad for the present study (Sø et al., 2011). These pre-existing models were developed using simple synthetic solutions, and we will adapt them for use with the complex electrolytes found in natural waters. To probe for the mechanism driving P dynamics of calcite immersed in these complex natural solutions, we combined laboratory experiments and geochemical modeling using geochemical software. We aimed to develop the first (to our knowledge) surface complexation model that can simulate P adsorption to calcite in natural freshwater. A surface complexation model of P dynamics for calcite in freshwater and seawater would be useful for projecting P fluxes in field settings.

2. Experimental procedures

2.1. Calcite

We used calcite from ACROS Organics that was reagent-grade (99+% pure). The specific surface area (0.68 $m^2\ g^{-1}$) was measured by N_2 Brunauer–Emmett–Teller (BET).

2.2. Solutions

To better approximate field conditions, we used two natural water types. We used a peristaltic pump to extract fresh groundwater (hereafter referred to as "freshwater") from the carbonate-based Floridan aquifer, from a well on the campus of University of South Florida, Tampa, FL, USA. To compare freshwater to contrasting natural water, we took a sample of seawater from the surface of the Gulf of Mexico near Fort DeSoto Park, St Petersburg, FL, USA. Since natural seawater is supersaturated with respect to calcite, we pre-equilibrated both solutions to calcite at a solid to solution ratio of 2 g L^{-1} overnight and filtered (0.2 μm) following Millero et al. (2001).

We found that even with pre-equilibrating our solutions to calcite as previously described, a subsequent addition of new calcite resulted in a decrease of solution pH, suggesting further calcite precipitation. To identify a calcite equilibrium condition in seawater under ambient atmospheric CO_2 (indoor condition), we approached the system from both ends, dissolution at low pH and precipitation at high pH, to locate a boundary condition where calcite neither dissolves nor precipitates in seawater. We conducted a series of preliminary batch experiments with 1 g calcite and 40 mL seawater (with and without pre-equilibration to calcite), in which we adjusted the initial pH of the solutions to cover a range from 7.0 to 11.0, equilibrated them overnight to calcite (with and without added P), and then measured the final pH. We found a crossover point at initial pH between 7.6 and 7.8 in seawater where ΔpH ≈0 (Fig. 1). Thus, to avoid calcite precipitation/dissolution, we used HCl to adjust both freshwater and seawater to pH = 7.7 prior to batch experiments. We also note that pH = 7.7 is ecologically relevant, since it is within the typical range of water in many coastal aquatic systems.

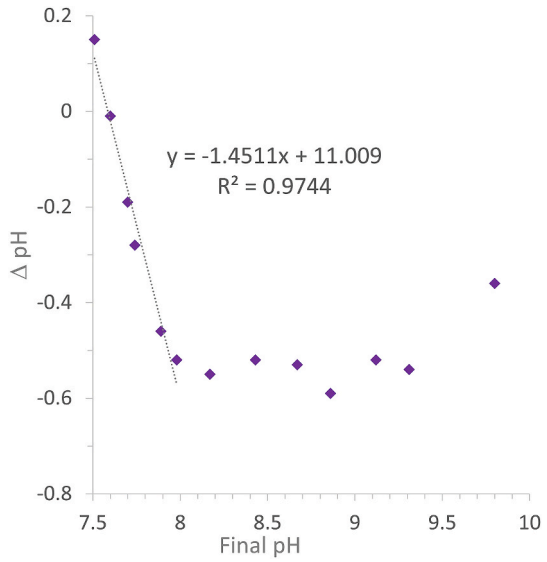

Fig. 1. Change in pH for seawater (that had previously been equilibrated with calcite and then filtered) that was adjusted to a range of initial pH with HCl, and then exposed to new calcite in a test tube for 24 h before being measured for final pH ($\Delta pH = pH_{final} - pH_{initial}$).

2.3. Major ionic components of waters

We measured conductivity and pH using a Thermo Scientific Orion Star A215 Benchtop pH/Conductivity Meter. Solution concentrations of Ca^{2+} and Mg^{2+} were measured by Inductively Coupled Plasma-Atomic Emission Spectrometry. Concentrations of SO_4^{2-} were measured by ion chromatography. We measured P concentrations in the solutions as soluble reactive phosphorus (SRP) by measuring absorbance at 630 nm in 96-well microplates on a BioTek EPOCH microplate spectrophotometer, using the microscale malachite green method (D'Angelo et al., 2001). The key characteristics of our freshwater and seawater (after pre-equilibration to calcite) are listed in Table 1.

2.4. Batch experiments

We studied phosphate adsorption using batch incubation methods adapted from Froelich (1988). We used 1.000 g calcite in 0.040 L solution, a surface to liquid ratio of 37.9 $m^2\ L^{-1}$. Stock solutions of phosphate (1 mM) were prepared with reagent grade Na_2HPO_4. To preserve the pH of our solutions after adding P, we adjusted the stock P solution to pH = 7.7. Phosphate was added to the batches to create 30 increments of initial P concentration ($[SRP]_i$) ranging from 2 μM to 60 μM (Millero et al., 2001). Triplicates were made at 32 μM P to evaluate analytical precision (coefficient of variation was 6.4% for seawater and 1.7% for freshwater). We added chloroform to inhibit microbial activity (Detenbeck and Brezonik, 1991). Tubes were incubated at room temperature on a platform shaker (200 rpm) for 24 h. Following this, each suspension was filtered using a 0.45 μm nylon syringe filter. An aliquot from each filtrate was then analyzed to measure the final SRP. Any loss of P from the solution under incubation condition is assumed to have been adsorbed to the mineral surface rather than apatite precipitation (see Appendix B for thorough discussion). The amount of P adsorbed on the calcite, ΔP_{ads} (μmol P g^{-1}), is calculated from the difference between initial SRP ($[SRP]_i$) and the final SRP ($[SRP]_f$) concentration, and normalized to 1 g of calcite and 1 L of solution:

$$\Delta P_{ads} = \left([SRP]_i - [SRP]_f\right) \times \frac{0.04\ L\ solution}{1g\ calcite} \quad (1)$$

where 1.000 g calcite and 40.0 mL solution used in the experiments were taken account in equation (1).

A plot of ΔP_{ads} vs. $[SRP]_f$ is used to describe the adsorption behavior of P with calcite when immersed in the two water types. The resulting curves are commonly referred to as isotherm curves, emphasizing the temperature dependency of the P adsorption dynamics represented.

2.5. Adsorption isotherm parameters

Fitting empirical data to Freundlich Isotherm and Two Surface Langmuir Isotherm equations can provide insights into overall aspects of P adsorption. We used log-weighted error to fit the parameters.

The Langmuir model is a theoretical approach that assumes the solid surface has a finite number of available adsorption sites, with adsorption reaching saturation at a maximum monolayer adsorption capacity or saturation concentration (P_{max}). Such behavior can be modeled as:

$$\Delta P_{ads} = \frac{K_{eq} P_{max} [SRP]_f}{\left(1 + K_{eq}[SRP]_f\right)} \quad (2)$$

where the constant K_{eq} (μM^{-1}) is related to the binding energy of the adsorption sites on the solid surface, and has also been described as the affinity of P for the surface in the given solution.

Equation (2) assumes that all adsorption sites on the surface have uniform bonding energies, but the surfaces of most solids are heterogeneous. Syers et al. (1973) and Fetter (1977) developed a test: in a plot of $[SRP]_f/\Delta P_{ads}$ vs. $[SRP]_f$, one line segment indicates one surface, and two line segments indicate two surfaces. The Langmuir Two-Surface Sorption Isotherm is written (Langmuir, 1918):

$$\Delta P_{ads} = \frac{K_{eq1} P_{max1} [SRP]_f}{\left(1 + K_{eq1}[SRP]_f\right)} + \frac{K_{eq2} P_{max2} [SRP]_f}{\left(1 + K_{eq2}[SRP]_f\right)} \quad (3)$$

where the Langmuir model of adsorption for a single surface (equation (2)) is expanded to accommodate adsorption at two surfaces (Holford et al., 1974). The two "surfaces" represent two types of adsorption site at the interface between the solid and aqueous phase (the physical differences between these two types of sites on the crystal lattice are explored further in section 5.1.). The first quantity on the product side represents the surface with the higher bonding energy, and each of the parameters in equation (1) are appended with the subscript 1. The second quantity (with subscript 2) represents the lower bond energy. In this model, P ions adsorb to both types of sites throughout the incubation, in proportion to the bonding energy of the unoccupied sites (Holford et al., 1974).

The Freundlich isotherm model is an empirical approach particularly suited to heterogeneous surfaces such as soils and minerals (Freundlich, 1906). The Freundlich Isotherm equation is given as:

$$\Delta P_{ads} = \left(K_f \times [SRP]_f^n\right) \quad (4)$$

The Freundlich exponent, n, accounts for the heterogeneity of the solid surface; it is a number between 0 and 1. The lower the exponent,

Table 1
Selected characteristics of the two field waters used in experiments.

Water Type	pH	Salinity psu	Ca^{2+} mM	Mg^{2+} mM	Na^{+} mM	Cl^{-} mM	SO_4^{2-} mM	Total Alkalinity as HCO_3^- mM
Freshwater	8.21	0.1	2.75	0.2	0.7	0.8	1.66	2.98
Seawater	8.05	40.0	9.75	49.3	521.1	606.7	10.4	2.43

the more pronounced is the flattening of the isotherm curve, i.e., a higher contrast between intense (steep) P adsorption initially (at a higher energy surface), followed by weak adsorption as those more limited sites become filled, and a greater proportion of adsorption occurs at lower energy sites (which flattens the curve). As n approaches 1, P adsorption approaches linearity (no difference between high and low energy sites). The Freundlich coefficient (K_f) is the relative adsorption capacity, or the relative rate of removal of phosphorus per unit increase in $[SRP]_i$ (Yakubu et al., 2008). The Freundlich coefficient (K_f) functions as a scalar of total adsorption, with higher coefficient values resulting in higher total P adsorption (ΔP_{ads}).

2.6. Computer modeling approach

2.6.1. Geochemical software

We used the geochemical modeling program PHREEQC (Version 3.6) (Parkhurst and Appelo, 1999, 2013). This program was developed by the United States Geological Survey (USGS) to simulate a broad range of aqueous geochemical batch-interactions including aqueous speciation, saturation index, dissolution/precipitation, and surface complexation. The program uses a thermodynamic database consisting of a wide range of data for equilibria among aqueous complexes and the solubility of solid phases, and it uses these to predict geochemical outcomes at equilibrium. The user can make any changes or additions to the thermodynamic data used for the simulations. We wrote code to simulate the procedures for our freshwater and seawater batch experiments (described in Section 2.4; full codes are provided in Appendix A), and made additions and adjustments to the thermodynamic database (described below in Sections 2.6.2-2.6.4). Output collected from PHREEQC included the predicted ΔP_{ads}, the distribution of surface complexes, the distribution of aqueous species, and the saturation index of apatite.

2.6.2. Equilibria at the surface of calcite

Surface complexation models (SCMs) are a quantitative thermodynamic approach that simulate chemical equilibria at the interface between a mineral and its surrounding solution. These chemical models account for the effects of variable chemical conditions and allow the user to compare the plausibility of alternative reactions (Goldberg et al., 2007). In SCMs, adsorption reactions are defined and given specific equilibrium (stability or affinity) constants, analogous to aqueous complexes in the bulk solution. The surface reactions also determine the charge at the mineral surface, which in turn affects adsorption reactions.

Various SCMs differ in how they conceptualize and quantify the electrical charge distribution between the mineral surface and the bulk solution. We used the Constant Capacitance Model (CCM), a quantitative approach to surface interactions that is thought to be particularly well-suited to modeling high ionic strength solutions such as seawater (Gao and Mucci, 2003). It also performs better for heterogeneous surfaces than some other models, such as CD-MUSIC (Zhou et al., 2005). Sø et al. (2011) presented an adjustment to PHREEQC code to approximate the CCM. As a starting point for our model, we used previous CCM models for adsorption to carbonates started by Van Cappellen et al. (1993), and further developed by Pokrovsky et al. (2000), Pokrovsky and Schott (2002), Hiorth et al. (2010), and Sø et al. (2011) (Table 2). The primary sites at the calcite surface are calcium (denoted as $> Ca^+$) and carbonate functional groups ($>CO_3^-$) in equal abundance (where the symbol $>$ is used to denote the polar $CaCO_3$ surface with a terminal Ca^+ or CO_3^-, being charge-balanced by the opposite end of the same $CaCO_3$ molecule in the crystal lattice). Calcium sites are broken into strong sites (denoted as $> sCa^+$) and weak sites ($>wCa^+$), and P adsorbs to these sites as $CaPO_4^-$, $CaHPO_4^0$, or HPO_4^{2-} in competition with CO_3^{2-}, HCO_3^-, SO_4^{2-}, and H_2O^0 in solution (Table 2). In addition, Ca^{2+}, Mg^{2+} and H^+ compete for the carbonate group adsorption sites ($>CO_3^-$). and at both strong and weak calcium adsorption sites, P (as $CaPO_4^-$ and either $CaHPO_4^0$, or HPO_4^{2-}) competes with CO_3^{2-}, HCO_3^-, SO_4^{2-}, and H_2O (Fig. 2).

Table 2
Summary of surface complexation reactions and associated affinity constants from published literature[a,b,c] for negatively charged sites ending with a carbonate group ($>CO_3^-$), strong positively charged sites ($>sCa^+$) and weak positively charged sites ($>wCa^+$) at the surface of calcite. The error interval corresponds to the 95% confidence level. Phosphate reactions with the calcite surface are listed as two alternative models in the bottom two sections, each consisting of four reactions, as developed by Sø et al. (2011) for calcite in calcium carbonate solutions.

Reaction	Log K
$>CO_3H = >CO_3^- + H^+$	-5.1 ± 0.03[a]
$>CO_3H + Ca^{2+} = >CO_3Ca^+ + H^+$	-1.7 ± 0.06[a]
$>CO_3H + Mg^{2+} = >CO_3Mg^+ + H^+$	-1.7 ± 0.06 [a]
$>sCaCO_3^- + H_2O = >sCaOH_2^+ + CO_3^{2-}$	-5.25 ± 0.03[a]
$>wCaCO_3^- + H_2O = >wCaOH_2^+ + CO_3^{2-}$	-5.25 ± 0.03
$>sCaCO_3^- + HCO_3^- = >sCaHCO_3 + CO_3^{2-}$	-3.929 ± 0.06[a]
$>wCaCO_3^- + HCO_3^- = >wCaHCO_3 + CO_3^{2-}$	-3.929 ± 0.06
$>sCaCO_3^- + SO_4^{2-} = >sCaSO_4 + CO_3^{2-}$	-3.15[b]
$>wCaCO_3^- + SO_4^{2-} = >wCaSO_4 + CO_3^{2-}$	-3.15
Model 1 from Sø et al. (2011)	
$>sCaCO_3^- + CaHPO_4^0 = >sCaHPO_4Ca^+ + CO_3^{2-}$	0.90 ± 0.06[c]
$>wCaCO_3^- + CaHPO_4^0 = >wCaHPO_4Ca^+ + CO_3^{2-}$	-1.75 ± 0.07
$>sCaCO_3^- + CaPO_4^- = >sCaPO_4Ca^0 + CO_3^{2-}$	2.21 ± 0.03
$>wCaCO_3^- + CaPO_4^- = >wCaPO_4Ca^0 + CO_3^{2-}$	-0.79 ± 0.07
Model 2 from Sø et al. (2011)	
$>sCaCO_3^- + HPO_4^{2-} = >sCaHPO_4^- + CO_3^{2-}$	0.17 ± 0.16[c]
$>wCaCO_3^- + HPO_4^{2-} = >wCaHPO_4^- + CO_3^{2-}$	-2.00 ± 0.15
$>sCaCO_3^- + CaPO_4^- = >sCaPO_4Ca^0 + CO_3^{2-}$	2.30 ± 0.05
$>wCaCO_3^- + CaPO_4^- = >wCaPO_4Ca^0 + CO_3^{2-}$	-0.72 ± 0.10

[a] Pokrovsky and Schott (2002).
[b] Hiorth et al. (2010).
[c] Sø et al. (2011).

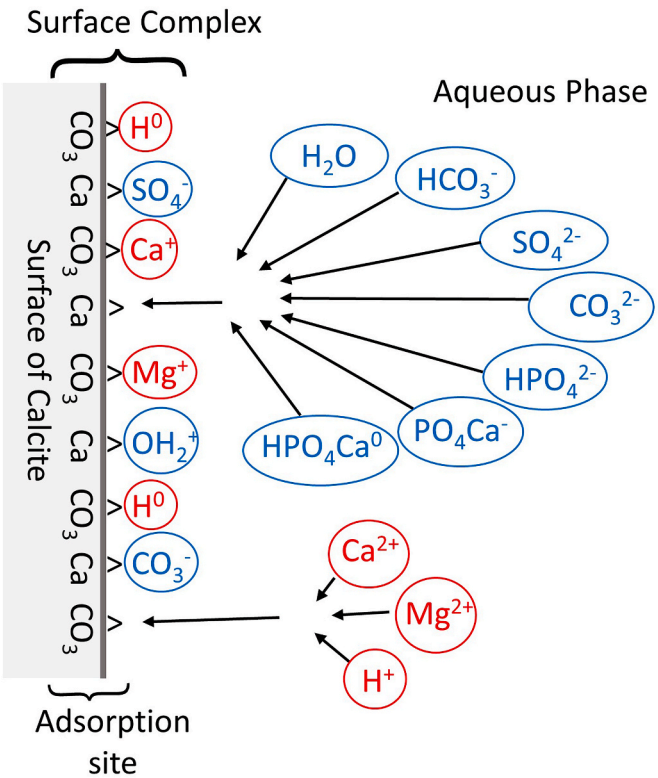

Fig. 2. Simplified, schematic representation of surface complexes. at the calcite/water interface at positive $> Ca^+$ and negative $> CO_3^-$ sites, partially based on illustrations by Gao and Mucci (2003) and Mahani et al. (2017).

We also tested a model that included cooperative adsorption between Mg^{2+}–P ion pairs and the surface, substituting Mg^{2+} for Ca^{2+} in the surface complexation models in the lower two sections of Table 2 as a

starting point.

One of the parameters that must be set is the ratio of strong to weak sites. According to Dzombak and Morel (1990), strong sites typically have lower density than weak sites. We adopted the total site density of 8.22 μmol/m^2 for both calcium and carbonate sites, and the ratio of strong:weak sites from Pokrovsky and Schott (2002) and Sø et al. (2011). The ratio of strong vs. weak sites determines the curvature of the isotherms; the fact that our modeled curves matched well with our experimental results suggests that this assumption was acceptable in this study.

Our efforts for the present study were directed at determining which of the previously published surface complexation reactions (Table 2) were necessary to reproduce our experimental data for the two water types, and to assign affinity constants to the selected P sorption reactions, specific to the water type. It is not possible to directly use previously published reactions and affinity constants to simulate reactions in freshwater and seawater, because affinity constants are specific to the physico-chemical characteristics of the mineral phase, solutions, and conditions of the experiments from which they were derived. Affinity constants developed in single or dual electrolyte solutions do not account for the competition that occurs in more complex solutions (Sø et al., 2008). No surface complexes or affinity constants have been developed for calcite or any mineral in seawater. The interdependency of the many adsorbing species make it impossible to calibrate surface complexes for several adsorbing species at once. To narrow down P surface reactions and to calibrate associated affinity constants, we used PEST (version 16.0), a computer program that offers model-independent parameter estimation and uncertainty analysis developed by Doherty (2004).

2.6.3. Calcite solubility

Calcite is more soluble in seawater than in pure water, and this must be taken into account when dissolution/precipitation of calcite is an important part of an experiment. For our freshwater experiments, we used the intrinsic calcite solubility ($K_{sp} = -8.48$) (Langmuir, 1968; Plummer and Busenberg, 1982). For our seawater experiments, we used the apparent solubility of calcite in seawater at 25 °C and 1 atm of pressure ($K_{sp}^* = -6.35$) (Morse et al., 1980).

2.6.4. Equilibria in solution

To model aqueous speciation in our freshwater solution, we used intrinsic association constants (K_{int}, from the database phreeqc.dat) (Table 3). We compared results with the phreeqc.dat database and another database (wateq.v4), and found no difference in predicted ΔP_{ads}. To model aqueous speciation in our seawater solution, we used apparent affinity constants for seawater at 25 °C (K*) (Table 3).

3. Experimental results and isotherm parameters

Our results showed that P adsorbed more to calcite in freshwater compared with seawater (Fig. 3a, Table 4; raw data is provided in Appendix A). The mean ΔP_{ads} in freshwater was 0.84 μmol P g^{-1}, compared to 0.59 μmol P g^{-1} in seawater. Based on our Freundlich Isotherm parameters, freshwater adsorption efficiency was 50% higher than seawater (Freshwater $K_f = 0.45$ L g^{-1} and Seawater $K_f = 0.30$ L g^{-1}; Table 4). The dimensionless Freundlich coefficient n was also much higher in freshwater (3.4) compared to seawater (2.8).

Our experimental data could best be represented as having two types of P adsorption sites with contrasting bonding energies (strong and weak). First, when plotted as $[SRP]_f/\Delta P_{ads}$ vs. $[SRP]_f$, the data for both water types exhibited two linear line segments, with the distinction being more pronounced in freshwater (Fig. 3b). Fitting the data for both water types to Equation (2) did not work well ($R^2 < 0.86$), the fit was much better ($R^2 \geq 0.96$) using the Langmuir Two-Surface Sorption Isotherm (Equation (3)). Two surfaces were sufficient to explain our empirical data with the minimal number of parameters.

Table 3
Stoichiometric aqueous complexation constants for K_{int} (from PHREEQC.dat database) and K* for seawater (25 °C) from the published literature [b, c].

Reactions	Log K_{int}	Seawater Log K*
$H_2O = OH^- + H^+$		−13.215[b]
$CO_3^{2-} + H^+ = HCO_3^-$	10.329[a]	8.95 [b]
$PO_4^{3-} + H^+ = HPO_4^{2-}$	12.34 [a]	21.721[b]
$PO_4^{3-} + 2H^+ = H_2PO_4^-$	19.553[a]	19.76[b]
$PO_4^{3-} + 3H^+ = H_3PO_4^0$	21.721[a]	16.337[b]
$Na^+ + HPO_4^{2-} = NaHPO_4^-$	0.29[a]	0.05[c]
$Na^+ + H_2PO_4^- = NaH_2PO_4$	absent	−0.54[c]
$Na^+ + PO_4^{3-} = NaPO_4^{2-}$	absent	0.52[c]
$Mg^{2+} + SO_4^{2-} = MgSO_4$	2.37 [a]	1.01[c]
$Mg^{2+} + H^+ + CO_3^{2-} = MgHCO_3^+$	11.399[a]	0.28[c]
$Mg^{2+} + CO_3^{2-} = MgCO_3$	2.98[a]	1.94[c]
$Mg^{2+} + H_2O = MgOH^+ + H^+$	−11.44[a]	−12.02[c]
$SO_4^{2-} + H^+ = HSO_4^-$	1.98[a]	1.49[c]
$Ca^{2+} + H_2O = CaOH^+ + H^+$	−12.7[a]	−12.98[c]
$Ca^{2+} + CO_3^{2-} = CaCO_3$	3.224[a]	2.1[c]
$Ca^{2+} + CO_3^{2-} + H^+ = CaHCO_3^+$	11.435[a]	0.33[c]
$Ca^{2+} + SO_4^{2-} = CaSO_4$	2.25[a]	1.03[c]
$Mg^{2+} + PO_4^{3-} = MgPO_4^-$	6.589[a]	3.84[c]
$Mg^{2+} + HPO_4^{2-} = MgHPO_4^0$	2.87[a]	1.51[c]
$Mg^{2+} + H_2PO_4^- = MgH_2PO_4^+$	1.513[a]	0.47[c]
$Ca^{2+} + PO_4^{3-} = CaPO_4^-$	6.45 [a]	4.5[c]
$Ca^{2+} + HPO_4^{2-} = CaHPO_4^0$	2.739[a]	1.28[c]
$Ca^{2+} + H_2PO_4^- = CaH_2PO_4^+$	1.408[a]	0.24[c]

[a] From PHREEQC.dat database.
[b] From Pierrot and Millero (2016).
[c] Millero and Schreiber (1982).

The saturation concentrations for both surfaces are much higher in freshwater than seawater (freshwater's P_{max1} of 0.68 μmol P g^{-1} is 2.8 times higher than seawater's P_{max1} of 0.24 μmol P g^{-1}, and freshwater's P_{max2} of 3.54 μmol P g^{-1} is 4.6 times higher than seawater's P_{max2} of 0.77 μmol P g^{-1}). The $k_{eq\ (1)}$ for seawater ten times higher (20.50 μM^{-1}) compared to freshwater (2.13 μM^{-1}). This may be an artifact of our experimental conditions, since this parameter is sensitive to the $[SRP]_f$ measurements of the first few low $[SRP]_f$ data points, which were very close to our detection limit. However, the $k_{eq\ (2)}$ is also higher for seawater (0.08 μM^{-1}) compared to freshwater (0.01 μM^{-1}).

4. Modeling results

4.1. Simulation of P dynamics

We developed models that quite closely matched our empirical ΔP_{ads} in seawater ($R^2 = 0.9973$) and freshwater ($R^2 = 0.9899$), as shown in Figs. 3a, and Fig. 4. For both water types, our best fits were obtained using only a single P species reacting with strong and weak calcium sites: $CaPO_4^-$ for freshwater and HPO_4^{2-} for seawater (Table 5). Inclusion of reactions for Mg^{2+}–P adsorbing at the calcite surface made no difference in total ΔP_{ads} predicted by our models. To see the effect of water type on the viability of the P adsorption reactions, we ran a simulation for the seawater solution but using the P adsorption reactions and Log K values calibrated for freshwater, and the predicted ΔP_{ads} was close to zero (not shown).

For seawater, our computer model predicted a less steep initial increase than the two isotherms (the steepness of the first five seawater data points was noted as a possible experimental artifact in Section 3), and a slightly greater ΔP_{ads} at high $[SRP]_f$. For freshwater, our computer model predicted slightly more ΔP_{ads} than the two isotherms, particularly at high $[SRP]_f$ (Fig. 3a).

4.2. Strong vs. weak calcium sites

Fig. 4 shows the relative proportion of P adsorption to strong and weak calcium sites for the two water types in our computer simulations.

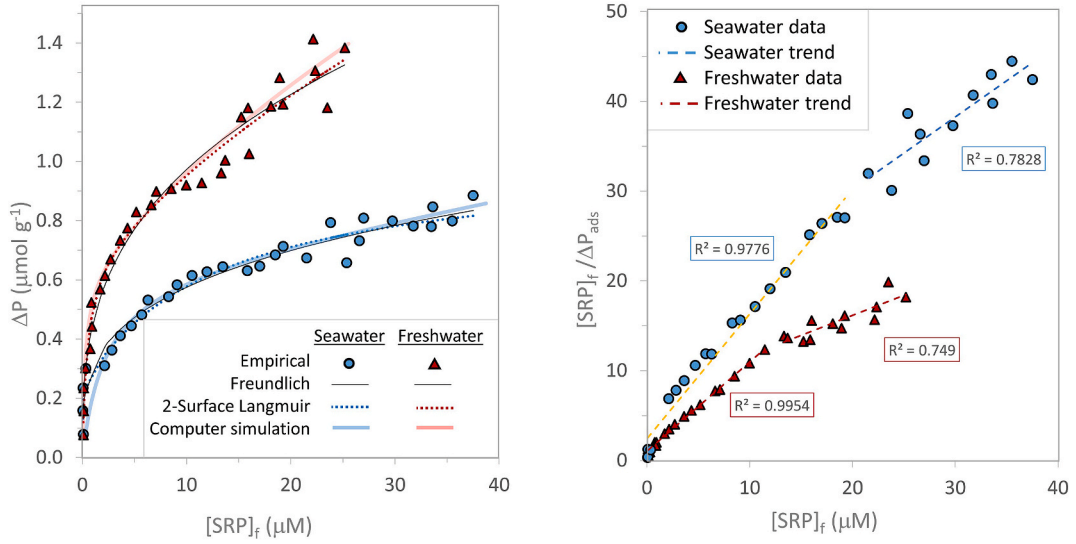

Fig. 3. Adsorption Isotherm Results. a) comparison among freshwater empirical results (black plus symbols), Freundlich Isotherm (thin black curve), Two-Surface Langmuir Isotherm (dotted red curve), and our computer simulation (solid pale red curve; discussed in Section 4.5 below); and the similar for seawater: seawater empirical results (green "x" symbols), Freundlich Isotherm (thin black curve), Two-Surface Langmuir Isotherm (dotted blue curve), and our computer simulation (solid pale blue curve); b) The linear plot of empirical data used to test whether there was more than one type of adsorption site. . (For interpretation of the references to colour in this figure legend, the reader is referred to the Web version of this article.)

Table 4
Phosphorus sorption characteristics for calcite with respect to the two water types.

Water type	Freundlich Parameters			Two-Surface Langmuir Parameters				
	K_f, L g^{-1}	n	R^2	P_{max1} μmol P g^{-1}	$K_{eq\ (1)}$ μM^{-1}	P_{max2} μmol P g^{-1}	$K_{eq\ (2)}$ μM^{-1}	R^2
Seawater	0.30	0.28	0.96	0.24	20.50	0.77	0.08	0.96
Freshwater	0.45	0.34	0.97	0.68	2.13	3.54	0.01	0.98

K_f Freundlich adsorption coefficient.
n Freundlich exponent, dimensionlessP_{max1} Adsorption maximum for the first surface sites.
$K_{eq\ (1)}$ Adsorption energy for the first surface sites.
P_{max2} Adsorption maximum for the second surface sites.
$K_{eq\ (2)}$ Adsorption energy for the second surface sites.

At $[SRP]_f < 1$ μM, almost all of the ΔP_{ads} was to strong calcium sites. As $[SRP]_f$ increased ($[SRP]_f \approx 1$ μM for freshwater, and $[SRP]_f \approx 5$ μM for seawater) the strong calcium sites approached saturation and P adsorption to calcite in seawater catches up, ending with only 4% more in freshwater ($\Delta P_{ads} = 0.612$ μmol P g^{-1} in freshwater vs. 0.588 μmol P g^{-1} in seawater; Fig. 4c). Meanwhile, P adsorption to the weak calcium sites continued to increase in a linear fashion (Fig. 4c). For most of the isotherm curve ($[SRP]_i \approx$ 5–60 μM) the steeper slope of P adsorption to the weak sites in freshwater vs. seawater drives the difference in total P adsorption between the two water types. For freshwater, P adsorption to weak calcium sites comes to exceed P adsorption to strong calcium sites starting at $[SRP]_f > 19$ μM, whereas in seawater P adsorption to weak calcium sites never exceeds 32% of total P adsorbed.

4.3. Distribution of surface sites

We evaluated the proportion of all surface complexes at strong and weak calcium sites, as well as at negative (carbonate) sites on the calcite surface, using $[SRP]_i = 60$ μM for comparison (Fig. 5). On strong calcium sites, P overwhelmingly dominates the surface in both Freshwater (99.5%), and seawater (95%). In freshwater, CO_3^{2-} adsorption to strong calcium sites is negligible (0.08%), whereas it is 4.5% of adsorption to strong calcium sites in seawater. In contrast, P occupies a minority of weak calcium sites in both freshwater (16%), and seawater (6%). Adsorption of CO_3^{2-} is much lower in freshwater compared to at both strong calcium sites (0.08% in freshwater, 4.5% in seawater) and weak calcium sites (13% in freshwater, 82% in seawater). More SO_4^{2-} adsorbs to weak sites in freshwater (17%) vs. seawater (2%). Adsorption of HCO_3^- is negligible for both site types and both water types, only reaching 1% of weak calcium sites in freshwater. At carbonate sites in freshwater, most were occupied by Ca^{2+} (45%) or unoccupied (49%), with a small amount of Mg^{2+} (6%). In seawater, Mg^{2+} dominated (76%), with the remainder being Ca^{2+} (21%) or unoccupied (3%).

We simulated a series of scenarios in PHREEQC to try to better understand the importance of certain ions in solution and their interactions with the surface. We found including surface reactions for SO_4^{2-}, Mg^{2+}, and Ca^{2+} made little difference in the predicted ΔP_{ads} (Fig. 6a; for reactions, see Appendix A). Specifically, omission of the SO_4^{2-} reactions produced less than 1% difference in ΔP_{ads}, and a slightly better fit to the experimental data ($R^2 = 0.9968$ without them, $R^2 = 0.9826$ with them).

The omission of Ca^{2+} surface complexes caused a slight overprediction of ΔP_{ads} (up to 3% at high P doses). The omission of the Mg^{2+} reactions produced up to 0.5% difference in ΔP_{ads}. Because the CO_3^{2-} surface complex is necessary in our script for P to adsorb, it was not possible to omit that complex from our simulations.

4.4. The role of aqueous species

Even without adsorbing to the surface, the presence of certain ions in solution can make a difference in P adsorption, due to changes in

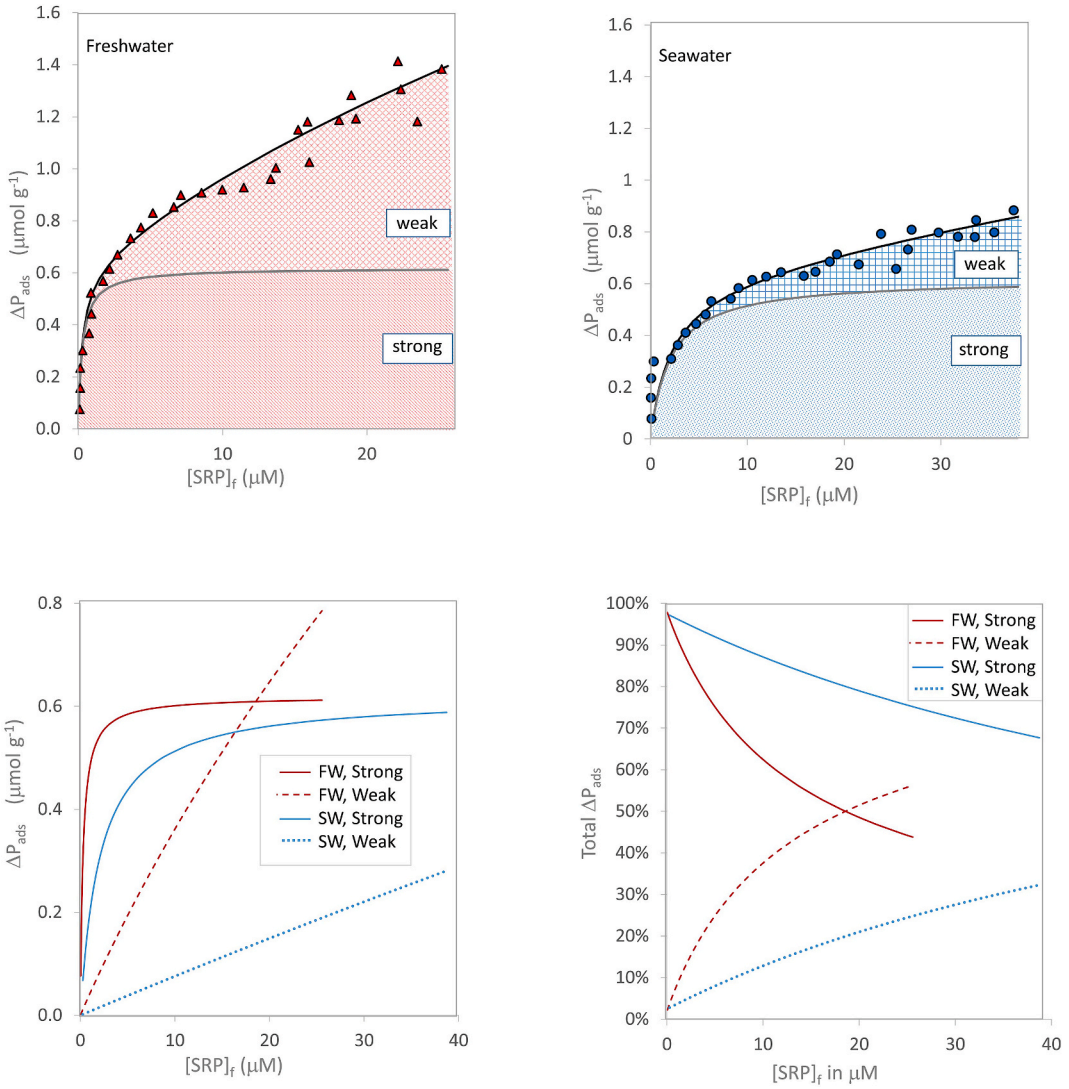

Fig. 4. Strong vs. weak calcium sites on the calcite surface for $CaPO_4^-$ in freshwater and HPO_4^{2-} in seawater; in the top row strong vs. weak calcium sites are indicated by shading and are shown additively, with total adsorbed P as a black curve, and empirical results shown as markers for a) freshwater (red triangles) and b) seawater (blue circles); in the bottom row the individual amount of P adsorption at strong (solid curves) vs. weak (dashed curves) is shown for freshwater (red) and seawater (blue), as an absolute concentration (c) and as a proportion of total P adsorbed (d). . (For interpretation of the references to colour in this figure legend, the reader is referred to the Web version of this article.)

Table 5
Our association constants for surface complexation reactions between P species and two kinds of positive sites (Ca) on the $CaCO_3$ surface. The error interval corresponds to the 95% confidence level.

Freshwater ($R^2 = 0.9899$)	**Log K**
$>sCaCO_3^- + CaPO_4^- = >sCaPO_4Ca^0 + CO_3^{2-}$	3.31 ± 0.33
$>wCaCO_3^- + CaPO_4^- = >wCaPO_4Ca^0 + CO_3^{2-}$	0.72 ± 0.02
Seawater ($R^2 = 0.9973$)	**Log K**
$>sCaCO_3^- + HPO_4^{2-} = >sCaHPO_4 + CO_3^{2-}$	1.98 ± 0.08
$>wCaCO_3^- + HPO_4^{2-} = >wCaHPO_4^- + CO_3^{2-}$	−0.51 ± 0.03
Number of carbonate sites $> CO_3^-$ (μmol m^{-2})	8.22
Number of strong calcium sites $> sCa^+$ (μmol m^{-2})	7.31
Number of weak calcium sites $> wCa^+$ (μmol m^2)	0.91

aqueous speciation. To explore the influence of solution composition on aqueous speciation and P adsorption, we ran simulations in which we doubled or omitted key ions from the seawater script (Fig. 6a and b). As with our changes in surface reactions, the differences were more pronounced at high $[SRP]_f$. Omitting NaCl increased the ΔP_{ads} by up to 81%, exceeding our freshwater empirical data. Doubling NaCl concentration had no effect. The effects of Mg^{2+} and Ca^{2+} ions were nearly mirror images of each other. Omitting Mg^{2+} ions increased ΔP_{ads} by up to 22%, and doubling Mg^{2+} concentration decreased ΔP_{ads} by up to 9%. Conversely, omitting Ca^{2+} ions decreased the ΔP_{ads} by up to 22%, and doubling Ca^{2+} concentration increased ΔP_{ads} by 16%. The omission of sulfate ions from the initial seawater solution resulted in almost no difference in simulated ΔP_{ads} (≤0.5%). The omission of total alkalinity (which mainly consists of $[HCO_3^-] + 2[CO_3^{2-}]$) from the initial seawater solution slightly over-predicted ΔP_{ads} (≤2%), and doubling its value slightly under-predicted ΔP_{ads} (≤2%).

Speciation of dissolved P species changes with elemental composition of solutions and thus can also make a difference in P adsorption. When compared to the distribution of P species in freshwater (Fig. 7a), our seawater (and standard seawater) had more HPO_4^{2-}, $NaHPO_4^0$ and $MgHPO_4^0$, and less $CaHPO_4^0$, $CaPO_4^-$, and $H_2PO_4^-$. Substituting a mean river water composition from Livingstone (1963) in place of our freshwater solution produced a ΔP_{ads} curve that diverged from our freshwater curve to eventually become more intermediate between our freshwater and seawater curves (Fig. 7b). There was negligible

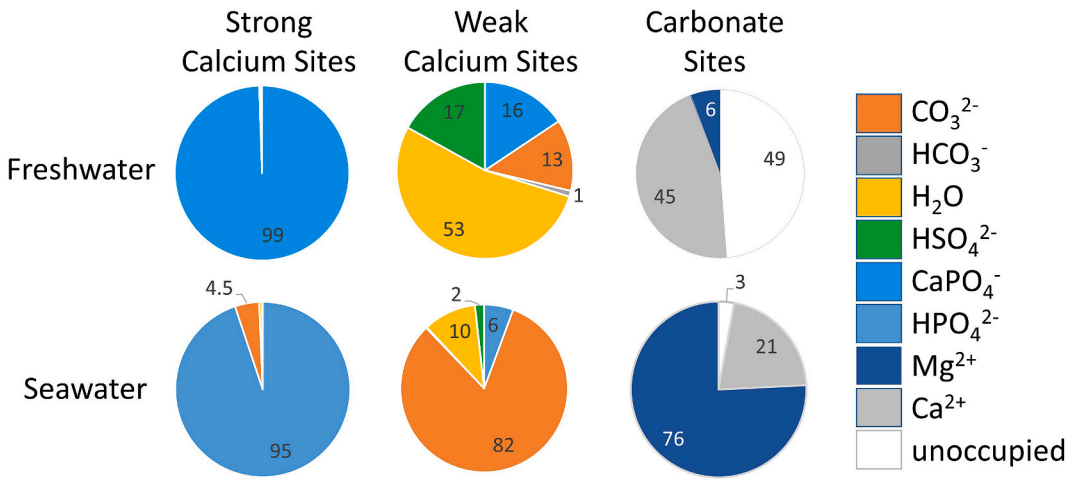

Fig. 5. The distribution of surface complexes. by water type (freshwater top row, seawater bottom row) and strong calcium sites (left hand column), weak calcium sites (center column), and carbonate sites (right hand column).

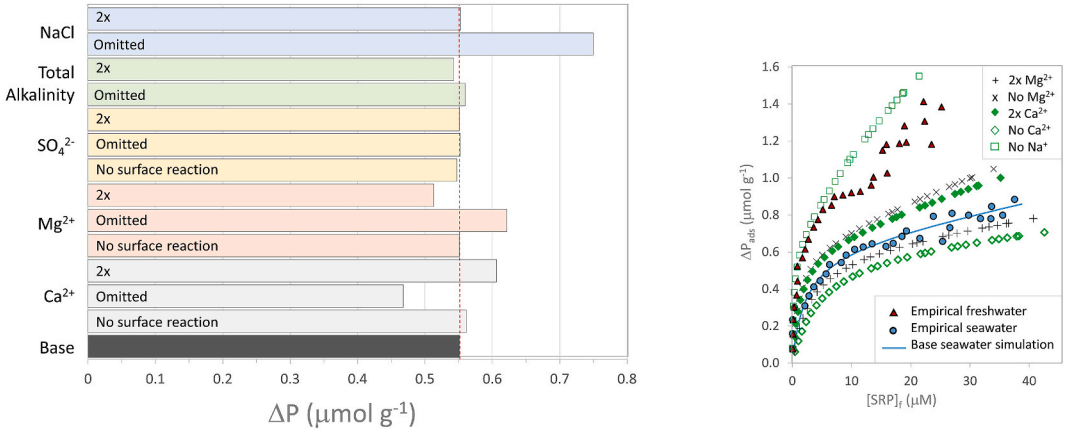

Fig. 6. The effect of various changes in our PHREEQC code on simulated ΔP_{ads}, compared to our empirical results (blue circles) and seawater model (solid blue curve), for. a) various alterations of initial seawater composition and surface reactions on ΔP_{ads} for $[SRP]_i = 24$ μM; b) the full simulated isotherms for doubling or omitting Mg^{2+} or Ca^{2+} from the initial seawater solution. . (For interpretation of the references to colour in this figure legend, the reader is referred to the Web version of this article.)

difference in ΔP_{ads} predicted for our seawater and the standard seawater.

5. Discussion

We developed the first (to our knowledge) geochemical models that simulates differential P adsorption to calcite in freshwater vs. seawater (Table 5, Figs. 2a and 4). Our models build on existing surface complexation reactions in the CCM and adapts them for the natural complex electrolyte solutions (Pokrovsky and Schott, 1999; Pokrovsky et al., 1999; Sø et al., 2011).

The purpose of this study is to better understand the underlying mechanism for strong P adsorption to calcite in freshwater by contrasting it with the same process in seawater. Our results suggest that the preferential P species adsorbing at positively charged calcium sites on the calcite surface differs depending on water type: $CaPO_4^-$ in freshwater and HPO_4^{2-} in seawater. The adsorption of HPO_4^{2-} is consistent with a sorption edge study of P adsorption to sediments from Taihu Lake, China (Zhou et al. (2005).

The surface reactions we used in our model (based on Sø et al. (2011)) are consistent with longstanding scientific consensus that P adsorption is typically specific (i.e., inner sphere, meaning that no water molecules are between the adsorption sites and the adsorbing anion) and further that P adsorption occurs via ligand exchange with anions (in our case, mainly carbonate) chemically bonded to metallic ions at the sorbent surface (in our case, calcium) (Goldberg and Sposito, 1985). Ligand exchange is highly selective as to the anions and can remove large proportions of anions even in quite dilute solutions with high concentrations of less selective anions (Loganathan et al., 2014). Spectroscopic investigation of P adsorption to hematite have supported the dominance of the inner sphere adsorption mechanism, while highlighting the variability of complexes based on pH and surface coverage (Elzinga and Sparks, 2007). This spectroscopic finding is consistent with our modeling observation that adsorbing P species alters depending on water type. Although spectroscopy was beyond the scope of this study, in the future it would be valuable to use spectroscopic techniques such as scanning electromicroscopy, X-ray absorption fine structure and Fourier-Transform infrared analysis to further explore the mechanism of P adsorption to calcite under a variety of water types and conditions.

Adsorption of P is sometimes accompanied by precipitation of calcium phosphate phases such as apatite (e.g., $Ca_5(PO_4)_3(OH)$), although we have reason to believe this process was negligible in our experiments. It is true that when aqueous P concentrations are much higher than ours and pH is high, crystalline phases of apatite (e.g., $Ca_5(PO_4)_3(OH)$) can substantially enhance removal of P from solution when the absorbent is calcium-enhanced biochar or calcite (Sø et al., 2011; Loganathan et al.,

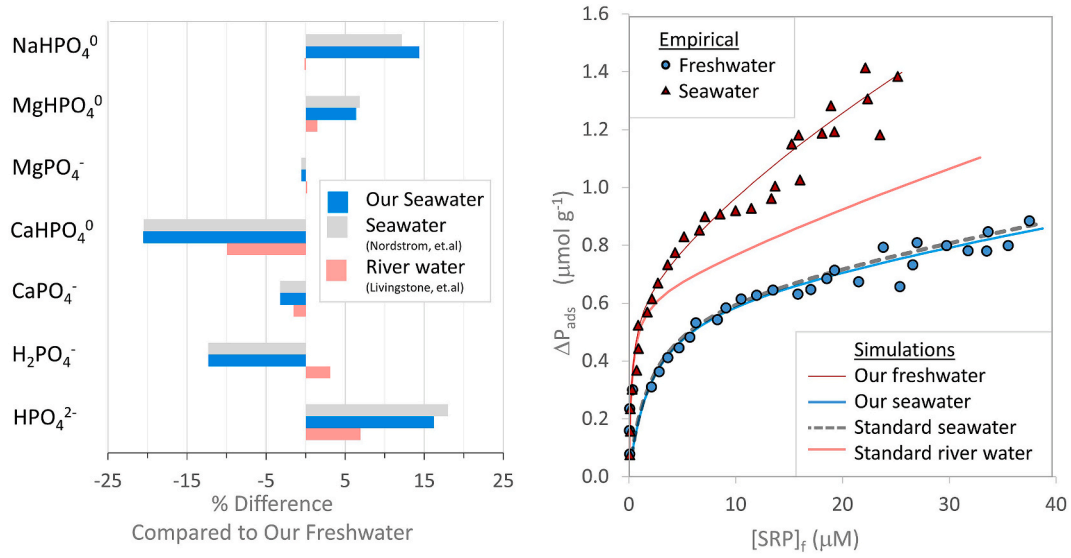

Fig. 7. a) P speciation in our freshwater compared to our seawater, a reference seawater from Nordstrom et al. (1979) and a reference river water composition from Livingstone (1963), presented as % difference compared to aqueous P speciation in our freshwater; b) predicted P adsorption for these reference water types compared to the freshwater and seawater used in this study.

2014; Wang et al., 2018). However, the low concentrations of aqueous P and the lower pH of our experiments make apatite precipitation unlikely, based on parameters outlined by Sø et al. (2011). Further, we conducted PHREEQC simulations of apatite precipitation in the context of our experiments (shown and discussed in Appendix B), and found that if precipitation had occurred, it would have occurred in certain of our seawater solutions and none of our freshwater solutions. Such precipitation would have been measured as heightened P removal (ΔP) in a few of our seawater solutions, whereas in our experiments much more P was removed from our freshwater solutions (Fig. 3). It is likely that the Mg^{2+} concentrations in our seawater inhibited the precipitation of calcium-phosphate phases, as has been observed in other studies (Salimi et al., 1985; Cao and Harris, 2008).

In Sections 5.1 and 5.2 below, we will discuss in detail further clues as to P dynamics at the calcite surface, and in Section 5.3 we will present our conceptual model.

5.1. *Different adsorption sites at the calcite surface*

In calcite, as for soils, it is generally necessary to consider more than one type of adsorption site (or "surface") with contrasting energies in order to adequately capture the interactions between dissolved constituents and the solid surface (Wolthers et al., 2012). Despite the array of different energies on the real calcite surface (described below), we found that dividing adsorption sites into just two types of sites (strong and weak) was sufficient to fit our empirical data well.

5.1.1. *Microscopic calcite adsorption sites*

Calcite crystal faces have different energy depending on whether they are terminated by both calcium and carbonate functional groups (low energy) or solely calcium or solely carbonate (high energy) (Sekkal and Zaoui, 2013). The dipole moment of polar faces makes them unstable, and adsorption of ions can neutralized the charge. Arguably the most important factors for determining calcite surface reactivity are corners and surface topography (Wolthers et al., 2012). Calcite crystals have perfect cleavage along rhombohedral planes in the crystal lattice, resulting in acute or obtuse angles where damage or other imperfections occur. The acute edges of stepped surfaces such as "etch pits" (depressions) and "islands" (plateaus) have much stronger charge than the obtuse angles.

5.1.2. *High vs. low energy sites in our surface complexation model*

Our simulations allow us to observe the shift as to which types of sites drive the greater P adsorption in both freshwater and seawater. Strong calcium sites drive P adsorption at low P concentrations (i.e., left-most side of graph, analogous to oligotrophic conditions) and weak calcium sites dominate at higher P concentration (above ~ 1–5 μM $[SRP]_f$, middle-to-right hand side of graphs, Fig. 4c and d). The strong sites are effective at attracting P, but they soon approach saturation at elevated solution P concentrations (Fig. 4c). At about the mid-point in Fig. 4d, adsorption of P to weak calcium sites comes to dominate total P adsorption in freshwater, whereas in seawater weak calcium sites never reach more than 1/3 of the total P adsorption.

5.1.3. *High vs. low energy sites in our Two-Surface Langmuir Isotherm*

The strong and weak calcium sites in our computer model correspond to the "high energy" and "low energy" surfaces in the Two-Surface Langmuir Isotherm as described by Holford et al. (1974) for soils. Like our thermodynamic model, the Langmuir Isotherm assumes two types of adsorption sites with monolayer adsorption (no stacking of adsorbates) that have a fixed number, and thus these sites can become saturated. The equation is derived from an equilibrium-approach to P adsorption analogous to solubility reactions.

Thus, our Langmuir isotherm parameters for the two surfaces (P_{max1}, $K_{eq\ (1)}$ for Surface 1, and P_{max2} and $K_{eq\ (2)}$ for Surface 2, Table 4) can be compared to strong vs. weak calcium sites on the calcite surface in Fig. 4. The Langmuir estimate of saturation concentration for the first surface in freshwater (P_{max1} = 0.68 μmol P g^{-1}) matches the corresponding value from our computer simulation (0.612 μmol P g^{-1}), estimated using the end point of the flattened solid red curve in Fig. 4c. For seawater the match is not as good; the computer simulated saturation (0.588 μmol P g^{-1}) is double the Langmuir estimate (0.24 μmol P g^{-1}), and we will argue that this can be explained by the role of P_{max} in determining the shape of the isotherms. (We were not able to use our computer simulation to estimate a saturation concentration since the trend of P adsorption to weak calcium sites is linear, shown as dashed lines in Fig. 4c).

We find that in our Langmuir isotherms, relative saturation concentrations (P_{max1} and P_{max2} for freshwater vs. seawater) drive their differences in ΔP_{ads}, and not the other parameters ($K_{eq\ (1)}$ and $K_{eq\ (2)}$). The saturation concentration at the first surface is almost three times higher in freshwater vs. seawater, and at the second surface it's almost a

factor of 5 (Table 4). In contrast, the relative binding energies ($K_{eq\ (1)}$ and $K_{eq\ (2)}$, also described as the affinity of P for the surface) are actually higher in seawater at both types of sites. These findings are consistent with a batch study of P adsorption to calcareous sediment in freshwater and seawater (Flower et al., 2016).

Further, since the solid material was the same for all of our experiments, the observed differences in saturation concentrations (P_{max1} and P_{max2}) between our freshwater and seawater data do not reflect the intrinsic adsorption site concentrations (although they would in studies comparing different sediments). Instead, differences in these parameters in the present study reflect the influence of water quality on the availability to P of adsorption sites on the calcite surface, by altering the concentrations of the preferred adsorbing P species, as well as the ability of P to compete with other ions for adsorption sites, and perhaps also altering kinetic factors.

5.1.4. High vs. low energy sites in our Freundlich Isotherm

Like the Langmuir isotherm, the Freundlich isotherm [Equation (4)] is also considered a good choice for heterogeneous surfaces, and it fits well with a wide range of adsorption data for minerals and soils. The Freundlich isotherm differs from the Langmuir in two key ways: (1) it assumes that the solid surface does not become saturated, since a power function with a fractional exponent does not converge, and thus does not have an upper limit or saturation concentration, and (2) it is empirically based, in contrast the theoretical basis of the Langmuir isotherm.

The influence of K_f, the coefficient of the power function, is most prominent in determining the initial steepness of the curve at low P concentrations (the left hand side of the graph). Plots of curves with the same K_f value (red vs. blue curves in Fig. 8) initially produce nearly the same ΔP_{ads} regardless whether the n was the freshwater value (solid curves) or the seawater value (dashed curves). Thus, K_f reflects the initial prominence of intense P adsorption at the first surface (the strong sites), closely relating it to P_{max1} in the Langmuir Two-Surface Isotherm, and the strong sites in our computer simulation (Fig. 4a and b). The Freundlich K_f has been described as the relative adsorption capacity, or the relative rate of removal of phosphorus per unit increase in $[SRP]_f$ (Yakubu et al., 2008).

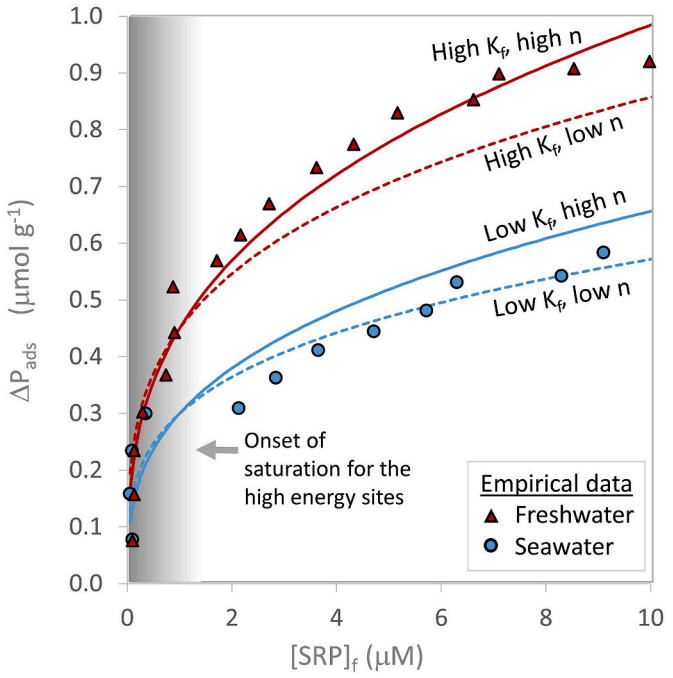

Fig. 8. The influence of Freundlich isotherm parameters, shown with empirical data for reference (red triangles for freshwater, blue circles for seawater), where curves bearing the "High" freshwater K_f are red and those bearing the "Low" seawater K_f are blue, and those bearing the "high" freshwater n are shown as solid curves, and the "low" seawater n as dashed curves. Our hypothesized transition between the prominence of the first and second surfaces is shown as gray vs. white background. . (For interpretation of the references to colour in this figure legend, the reader is referred to the Web version of this article.)

There is a clear point when the influence of the Freundlich exponent n causes curves with the same K_f to diverge. The point of divergence may roughly reflect the increasing importance of the second, lower energy surface, due to the first surface starting to become saturated. The lower the fractional exponent n, the shallower the slope in the subsequent part of the curve. Although the Freundlich exponent n has been described as representing the bond strength between P and the surface (Yakubu et al., 2008), this interpretation may be most relevant when comparing the P adsorption to solids with different characteristics. For our experimental data, the fractional exponent n closely relates to the diminished site availability for P at the lower energy surface, corresponding to (P_{max1}) of the Langmuir Two-Surface Isotherm.

5.1.5. Three ways to model high vs. low energy sites on calcite

In the preceding sections we have shown that P dynamics at the heterogeneous calcite surface are accounted for with distinct parameters for the high vs. low energy adsorption sites in our three different approaches to predicting/describing P adsorption to calcite, and that all of these are higher in freshwater vs. seawater (Tables 4 and 5). This allows us to draw connections between these heretofore disparate systems, shown in Table 6.

5.2. Solution composition: effects on surface charge and P adsorption

Dissolved ions in solution can trigger differential behavior of P at the calcite surface in seawater vs. freshwater. In a study of electrokinetics at the solid-solution interface of calcite Mahani et al. (2017) measured the ζ-potential at the surface of different types of carbonate rock immersed in a variety of chemical solutions. They found the divalent ions Ca^{2+} and CO_3^{2-} to be the most important for determining calcite surface charge, dubbing them the "potential-determining ions" (Mahani et al., 2017). The monovalent ions and H^+ and OH^- are secondary due to their lower concentrations in seawater compared to the major seawater ions, while Na^+ and K^+ were found to have little or no effect on calcite surface properties, suggesting little adsorption to the surface (Mahani et al., 2017).

The effect of increasing concentrations of Ca^{2+} and Mg^{2+} in solution is to make the calcite surface increasingly positive (Zhang and Austad, 2006; Mahani et al., 2017). In batch experiments, Millero et al. (2001) found that these cations enhanced P adsorption when added to NaCl solutions. They suggested that Ca^{2+} and Mg^{2+} facilitate P adsorption through bridged reactions, or through the adsorption of Ca^{2+}-P or Mg^{2+}-P ion pairs. Our scenarios indicate enhanced P adsorption with increased Ca^{2+} concentration (Fig. 6a and b). Doubling concentration of Ca^{2+} in the initial seawater solution strongly enhanced ΔP_{ads} (by up to 16%); and omitting these ions in the initial seawater solution decreased ΔP_{ads} (by up to 22%). Since HPO_4^{2-} is the sole adsorbing P species in our seawater model, it is not clear how Ca^{2+} enhances P adsorption within

Table 6
Our conceptual model of how the heterogeneity of the calcite surface is accounted for in the various approaches to predicting/describing P adsorption. All of these six parameters are higher in freshwater compared to seawater in this study.

	High energy sites	Low energy sites
Surface complexation Model	Log K for P adsorption at > sCa^+	Log K for P adsorption at > wCa^+
Langmuir Two-Surface Isotherm	P_{max1}	P_{max2}
Freundlich Isotherm	K_f	n

that model.

Conversely, Mg^{2+} has the opposite effect: doubling Mg^{2+} ions in our initial seawater solution diminished ΔP_{ads} by 9%, and omitting them increased the ΔP_{ads} by up to 22%. (Fig. 6a and b). We were not able to develop a successful model involving the adsorption of Mg^{2+}-P ion pairs. The role of seawater Mg^{2+} and Na^{+} in our simulations is to strongly inhibit P adsorption by forming aqueous complexes with P. Compared to our freshwater, our seawater has much more $MgHPO_4^0$, $NaHPO_4^0$, and HPO_4^{2-}, and much less $CaHPO_4^0$, $CaPO_4^-$, and $H_2PO_4^-$ (Fig. 7a). The change in P speciation causes HPO_4^{2-} to be the preferred adsorbing P species in seawater, as opposed to $CaPO_4^-$ in freshwater. The greater availability of $CaPO_4^-$ to adsorb to calcite in freshwater due to lower concentrations of Mg^{2+} and Na^{+} may be a key driver of increased P adsorption in freshwater vs. seawater.

Although less has been said in the literature about Na^{+} inhibiting P adsorption, there is longstanding support in the literature for Mg^{2+} ions decreasing P adsorption by forming Mg^{2+}-P ion pairs, thereby inhibiting the formation of Ca^{2+}-P ion pairs that might otherwise adsorb to the surface (Leckie and Stumm, 1970; Kitano et al., 1978; Kuo and Mikkelsen, 1979; Yadav et al., 1984; Shariatmadari and Mermut, 1999). The influence of Mg^{2+} does not have to do with its interactions at the calcite surface in our model. Even though Mg^{2+} fills 76% of the carbonate sites in seawater (Fig. 4c), removing the Mg^{2+} surface complex ($>CO_3Mg^{+}$) from the script did not make much difference in the predicted ΔP_{ads} (Fig. 6a).

Oxyanions can inhibit P adsorption through an alternative route. Divalent anions like SO_4^{2-} make the surface more negatively charged (Zhang and Austad, 2006). In batch studies with aragonite (a polymorph of calcite) in NaCl solutions, the tendency of Ca^{2+} and Mg^{2+} to enhance P adsorption to aragonite was diminished with the addition of SO_4^{2-}, or CO_3^{2-}/HCO_3^- at seawater strength (Millero et al., 2001). Millero et al. (2001) proposed that HCO_3^- was the primary driver of diminished P adsorption to aragonite in seawater. In two different studies using batch experiments with low salinity solutions, an increase in HCO_3^- concentration resulted in a decrease in P adsorption to $CaCO_3$ (Millero et al., 2001; Sø et al., 2011). Further, in batch studies with aragonite in solutions across a range of salinities, P adsorption remained nearly the same when HCO_3^- concentration was held constant (at 2 mM) (Millero et al., 2001).

Based on these observations, Millero et al. (2001) predicted that if freshwater in a given region had higher HCO_3^- concentrations than seawater, less P would absorb to sediment particles in such freshwater compared to seawater. Flower et al. (2016) supported this hypothesis when they reported less P adsorption to calcareous sediment when immersed in a brackish groundwater with unusually high total alkalinity (presumed to mainly consist of HCO_3^-/CO_3^{2-}) vs. when immersed in full strength natural seawater with lower total alkalinity. However, the experiments in the present study do not support the hypothesis that higher total alkalinity *per se* is a primary driver of diminished P adsorption in seawater vs. freshwater. Despite the fact that total alkalinity was higher in our freshwater solution compared to our seawater (Table 1), our freshwater solutions still produced markedly higher P adsorption than our seawater solutions (Fig. 3a). In freshwater (compared to seawater) calcite exhibited higher adsorption capacity (K_f), higher bond strength (n), higher saturation concentrations (P_{max1} and P_{max2}), and higher Log K's (Tables 2 and 3). When we simulated double total alkalinity in our initial seawater solution, this only very slightly reduced predicted ΔP_{ads}, and omitting initial seawater total alkalinity altogether only slightly increased predicted ΔP_{ads} (Fig. 6a).

Even when CO_3^{2-} concentrations are low, these ions still cause more P to adsorb in freshwater compared to seawater. The distribution of surface complexes (Fig. 5) shows that even though our freshwater has 22% higher total alkalinity (Table 1), the calcite surface has 40 times less CO_3^{2-} adsorbed at strong calcium sites in freshwater compared to seawater, and only a quarter of the CO_3^{2-} adsorbed at weak calcium sites. An obscure aspect of the thermodynamics of the seawater solution appears to enhance the competitive edge of CO_3^{2-} against P at both types of calcium sites.

It is worth noting that CO_3^{2-} domination of the weak calcium sites in seawater occurs despite the fact that HCO_3^- is the much more abundant dissolved carbonate species at the pH we used for both our solutions (pH = 7.7). Although our model includes surface reactions for HCO_3^- at both strong and weak calcium sites (Table 3), HCO_3^- never adsorbs to more than 0.4% of strong calcium sites, or 4% of weak calcium sites. Pokrovsky and Schott (2002) determined that the Log K for HCO_3^- substituting for CO_3^{2-} at calcium sites was quite low (−3.929), strongly favoring the CO_3^{2-} (Table 3). A recent study has shown that CO_3^{2-} can be the dominant species of inorganic carbon at the calcite surface even when HCO_3^- is the dominant species in the solution (i.e., $7.5 < pH < 10.35$) (Andersson et al., 2016).

Sulfate does not appear to influence ΔP_{ads} in our simulations. We saw no change in the predicted ΔP_{ads} when we doubled or eliminated SO_4^{2-} ions in the initial seawater solution, nor when we omitted the sulfate surface reaction (Fig. 5a). It's interesting to note that sulfate occupied on weak calcium sites is four times more in freshwater than that in seawater (Fig. 5), despite the fact that seawater has six times more sulfate than the freshwater (Table 1). Apparently, seawater chemistry allows CO_3^{2-} to outcompete SO_4^{2-} as well as P at weak sites. The accumulating literature that shows SO_4^{2-} as a driver of diminished P adsorption involves soils undergoing microbially mediated sulfate reduction and the formation of iron sulfides (Caraco et al., 1989; Roden and Edmonds, 1997; Lamers et al., 1998; Lucassen et al., 2004; Zak et al., 2006). There is little if any evidence in literature for an abiotic process whereby SO_4^{2-} drives diminished P adsorption.

5.3. The mechanism for strong P adsorption in freshwater

As laid out in Sections 5.1 and 5.2, the significantly greater ΔP_{ads} in freshwater vs. seawater appears to be driven mainly by three factors:

1) The adsorbing P species in freshwater ($CaPO_4^-$) is more thermodynamically favorable than the adsorbing P species in seawater (HPO_4^{2-}) (Table 3).
2) Freshwater has high concentrations $CaPO_4^-$ (Fig. 7a). In seawater, the high concentrations of Na^{+} and Mg^{2+} drive aqueous P speciation to $NaHPO_4^0$ and $MgHPO_4^0$, which may scavenge P from the surface, and also makes $CaPO_4^-$ too scarce to adsorb in appreciable amounts (Fig. 7).
3) P more effectively competes with CO_3^{2-} for adsorption sites at the calcite surface in freshwater, even when the CO_3^{2-} concentration is high. In seawater, CO_3^{2-} ions outcompete all other ions (i.e., HPO_4^{2-}, SO_4^{2-}, and H_2O) at weak calcium sites (Fig. 5). The enhanced favorability of CO_3^{2-} surface complexes in seawater is due to the thermodynamics of seawater chemistry.

If a main driver of stronger P adsorption in freshwater vs. seawater arises more from the aqueous chemistry than specific surface reactions, this may help explain why the phenomenon is nearly ubiquitous globally, across wide-ranging lithologies.

5.4. Limitations

Any model is a simplification of the real world, and one must understand it and apply it within its limitations. The fact that our model fits the data well does not mean that its explanation is correct, only that it is internally consistent between our laboratory measurements and published thermodynamic data for relevant components of the system, within the code that we used. Some of the limitations in our study include that we focused our experiments on the influence of water composition between freshwater and seawater under benchtop (oxic) conditions with biological activity suppressed (with chloroform). We also recognize that myriad physicochemical factors influence P

adsorption capacity, such as pH and redox (Pant and Reddy, 2001; McDonald et al., 2019). Second, we employed many simplifying assumptions in order to code our model. For example, we made assumptions about the nature of the calcite surface, including that P adsorbs to calcium sites (rather than carbonate sites), and that there are two main types of calcium sites (strong and weak).

6. Conclusions

The strength of P adsorption to soils and sediments in freshwater drives P limitation in many freshwater aquatic systems (Paludan and Morris, 1999; Vitousek et al., 2010). The high capacity of sediment to adsorb P in freshwater also has important implications for coastal areas, because suspended sediment with adsorbed P is transported to estuaries where contact with seawater causes it to be released (Froelich, 1988). The process of P adsorption has also proven important in a variety of decontamination efforts such as sewage remediation and the extraction of pollutants such as uranium from wastewater (Kong et al., 2020). This paper demonstrates how geochemical thermodynamic simulations can be used to develop complexation models that can help explain differential P adsorption to calcite in seawater vs. freshwater. Our surface complexation model for P adsorption to calcite in freshwater and seawater is an important step forward in predicting the role that sediment can play in the coming decades, as freshwater areas become increasingly polluted with P, and sea level rise brings increasing seawater into previously freshwater regions. The model provided in this study could be used as a basis for modeling P remediation in freshwater and seawater field conditions, as well as the fate of P adsorbed in freshwater and estuarine wetlands.

Author contribution

Hilary Flower: Conceptualization, Methodology, Software, Formal analysis, Investigation, Writing – original draft, Writing – review & editing, Visualization, Supervision; Mark Rains: Funding acquisition, Writing – review & editing; Yasemin Taşcı; : Software; Jia-Zhong Zhang: Conceptualization, Methodology, Writing – review & editing, Kenneth Trout: Software; David Lewis: Funding acquisition, Writing – review & editing; Arundhati Das: Formal analysis, Investigation, Visualization; Robert Dalton: Formal analysis, Investigation

Declaration of competing interest

The authors declare that they have no known competing financial interests or personal relationships that could have appeared to influence the work reported in this paper.

Acknowledgements

We appreciate Annie Majette, Paulina Ramirez, Andre Rives, and William Westerfield for laboratory support, Cody Stephens for coding support, Dr. Eloy Martinez for providing laboratory equipment, and we are grateful to the Rains Ecohydrology Lab group at USF Tampa, especially Leanne Stepchinski and Dr. Kai Rains, for editorial comments, and Dr. Scott Campbell for recruiting interns. This manuscript has benefited from the thoughtful comments of reviewers. The scientific results and conclusions, as well as any views or opinions expressed herein, are those of the authors and do not necessarily reflect the views of NOAA or the Department of Commerce. This material is based upon work supported by the National Science Foundation through the Florida Coastal Everglades Long-Term Ecological Research program under Cooperative Agreements #DEB-2025954 and DEB1832229.

Appendix A. Supplementary data

Supplementary data to this article can be found online at https://doi.org/10.1016/j.chemosphere.2021.131596.

References

Andersson, M.P., Rodriguez-Blanco, J., Stipp, S.L.S., 2016. Is bicarbonate stable in and on the calcite surface? Geochem. Cosmochim. Acta 176, 198–205.
Brandano, M., Frezza, V., Tomassetti, L., Cuffaro, M., 2009. Heterozoan carbonates in oligotrophic tropical waters: the Attard member of the lower coralline limestone formation (Upper Oligocene, Malta). Palaeogeogr. Palaeoclimatol. Palaeoecol. 274, 54–63.
Cao, X., Harris, W., 2008. Carbonate and magnesium interactive effect on calcium phosphate precipitation. Environ. Sci. Technol. 42, 436–442.
Caraco, N., Cole, J., Likens, G., 1989. Evidence for Sulphate-Controlled Phosphorus Release from Sediments of Aquatic Systems.
D'Angelo, E., Crutchfield, J., Vandiviere, M., 2001. Rapid, sensitive, microscale determination of phosphate in water and soil. J. Environ. Qual. 30, 2206–2209.
de Kanel, J., Morse, J.W., 1978. The chemistry of orthophosphate uptake from seawater on to calcite and aragonite. Geochem. Cosmochim. Acta 42, 1335–1340.
Detenbeck, N.E., Brezonik, P.L., 1991. Phosphorus sorption by sediments from a soft-water seepage lake. 1. An evaluation of kinetic and equilibrium models. Environ. Sci. Technol. 25, 395–403.
Doherty, J., 2004. PEST Model-independent Parameter Estimation User Manual, vol. 3338. Watermark Numerical Computing, Brisbane, Australia, p. 3349.
Dzombak, D.A., Morel, F.M., 1990. Surface Complexation Modeling: Hydrous Ferric Oxide. John Wiley & Sons.
Elzinga, E.J., Sparks, D.L., 2007. Phosphate adsorption onto hematite: an in situ ATR-FTIR investigation of the effects of pH and loading level on the mode of phosphate surface complexation. J. Colloid Interface Sci. 308, 53–70.
Fetter, C., 1977. Attenuation of waste water elutriated through glacial outwash. Groundwater 15, 365–371.
Filippelli, G.M., 2008. The global phosphorus cycle: past, present, and future. Elements 4, 89–95.
Flower, H., Rains, M., Lewis, D., Zhang, J.-Z., Price, R., 2016. Control of phosphorus concentration through adsorption and desorption in shallow groundwater of subtropical carbonate estuary. Estuar. Coast Shelf Sci. 169, 238–247.
Freundlich, H., 1906. Freundlich's adsorption isotherm. Phys. Chem. 57, 384.
Froelich, P.N., 1988. Kinetic control of dissolved phosphate in natural rivers and estuaries: a primer on the phosphate buffer mechanism1. Limnol. Oceanogr. 33, 649–668.
Gao, Y., Mucci, A., 2003. Individual and competitive adsorption of phosphate and arsenate on goethite in artificial seawater. Chem. Geol. 199, 91–109.
Garing, C., Luquot, L., Pezard, P., Gouze, P., 2013. Geochemical investigations of saltwater intrusion into the coastal carbonate aquifer of Mallorca, Spain. J. Appl. Geochem. 39, 1–10.
Goldberg, S., Criscenti, L.J., Turner, D.R., Davis, J.A., Cantrell, K.J., 2007. Adsorption–desorption processes in subsurface reactive transport modeling. Vadose Zone J. 6, 407–435.
Goldberg, S., Sposito, G., 1985. On the mechanism of specific phosphate adsorption by hydroxylated mineral surfaces: a review. Commun. Soil Sci. Plant Anal. 16, 801–821.
Hiorth, A., Cathles, L., Madland, M., 2010. The impact of pore water chemistry on carbonate surface charge and oil wettability. Transport Porous Media 85, 1–21.
Holford, I., Wedderburn, R., Mattingly, G., 1974. A Langmuir two-surface equation as a model for phosphate adsorption by soils. J. Soil Sci. 25, 242–255.
Hou, E., Luo, Y., Kuang, Y., Chen, C., Lu, X., Jiang, L., Luo, X., Wen, D., 2020. Global meta-analysis shows pervasive phosphorus limitation of aboveground plant production in natural terrestrial ecosystems. Nat. Commun. 11, 1–9.
Kitano, Y., Okumura, M., Idogaki, M., 1978. Uptake of phosphate ions by calcium carbonate. Geochem. J. 12, 29–37.
Kogure, T., Aoki, H., Maekado, A., Hirose, T., Matsukura, Y., 2006. Effect of the development of notches and tension cracks on instability of limestone coastal cliffs in the Ryukyus, Japan. Geomorphology 80, 236–244.
Kong, L., Ruan, Y., Zheng, Q., Su, M., Diao, Z., Chen, D., Hou, L.a., Chang, X., Shih, K., 2020. Uranium extraction using hydroxyapatite recovered from phosphorus containing wastewater. J. Hazard Mater. 382, 120784.
Kuo, S., Mikkelsen, D., 1979. Effect of magnesium on phosphate adsorption by calcium carbonate. Soil Sci. 127, 65–69.
Lamers, L.P., Tomassen, H.B., Roelofs, J.G., 1998. Sulfate-induced eutrophication and phytotoxicity in freshwater wetlands. Environ. Sci. Technol. 32, 199–205.
Langmuir, D., 1968. Stability of calcite based on aqueous solubility measurements. Geochem. Cosmochim. Acta 32, 835–851.
Langmuir, I., 1918. The adsorption of gases on plane surfaces of glass, mica and platinum. J. Am. Chem. Soc. 40, 1361–1403.
Leckie, J.O., Stumm, W., 1970. Phosphate precipitation. Water Resour. Symp. 3, 237–249.
Lee, S.S., Heberling, F., Sturchio, N.C., Eng, P.J., Fenter, P., 2016. Surface charge of the calcite (104) terrace measured by Rb+ adsorption in aqueous solutions using resonant anomalous X-ray reflectivity. J. Phys. Chem. C 120 (28), 15216–15223.
Livingstone, D.A., 1963. Chemical Composition of Rivers and Lakes. US Government Printing Office.
Loganathan, P., Vigneswaran, S., Kandasamy, J., Bolan, N.S., 2014. Removal and recovery of phosphate from water using sorption. Crit. Rev. Environ. Sci. Technol. 44, 847–907.
Lucassen, E., Smolders, A., Van de Crommenacker, J., Roelofs, J., 2004. Effects of stagnating sulphate-rich groundwater on the mobility of phosphate in freshwater wetlands: a field experiment. Arch. Hydrobiol. 160, 117–131.

Mahani, H., Keya, A.L., Berg, S., Nasralla, R., 2017. Electrokinetics of carbonate/brine interface in low-salinity waterflooding: effect of brine salinity, composition, rock type, and pH on ζ-potential and a surface-complexation model. SPE J. 22, 53–68.
McDonald, G.J., Norton, S.A., Fernandez, I.J., Hoppe, K.M., Dennis, J., Amirbahman, A., 2019. Chemical controls on dissolved phosphorus mobilization in a calcareous agricultural stream during base flow. Sci. Total Environ. 660, 876–885.
Millero, F., Huang, F., Zhu, X., Liu, X., Zhang, J.-Z., 2001. Adsorption and desorption of phosphate on calcite and aragonite in seawater. Aquat. Geochem. 7, 33–56.
Millero, F.J., Schreiber, D., 1982. Use of the ion pairing model to estimate activity coefficients of the ionic components of natural waters. Am. J. Sci. 282, 1508–1540.
Morse, J.W., Mucci, A., Millero, F.J., 1980. The solubility of calcite and aragonite in seawater of 35%. salinity at 25 C and atmospheric pressure. Geochem. Cosmochim. Acta 44, 85–94.
Morse, J.W., Zullig, J.J., Bernstein, L.D., Millero, F.J., Milne, P., Mucci, A., Choppin, G. R., 1985. Chemistry of calcium carbonate-rich shallow water sediments in the Bahamas. J Am. J. Sci. 285.
Nordstrom, D., Plummer, L., Wigley, T., Wolery, T., Ball, J.W., Jenne, E., Bassett, R., Crerar, D., Florence, T., Fritz, B., 1979. A comparison of computerized chemical models for equilibrium calculations in aqueous systems. In: Jenne, E.A. (Ed.), Chemical Modeling in Aqueous Systems, Speciation, Sorption, Solubility, and Kinetics. ACS Publications, pp. 857–892.
Paludan, C., Morris, J.T., 1999. Distribution and speciation of phosphorus along a salinity gradient in intertidal marsh sediments. Biogeochemistry 45, 197–221.
Pant, H., Reddy, K., 2001. Phosphorus sorption characteristics of estuarine sediments under different redox conditions. J. Environ. Qual. 30, 1474–1480.
Parkhurst, D.L., Appelo, C., 2013. Description of input and examples for PHREEQC version 3: a computer program for speciation, batch-reaction, one-dimensional transport, and inverse geochemical calculations U.S. Geological Survey Techniques and Methods No. 6-A43. US Geological Survey.
Parkhurst, D.L., Appelo, C.J., 1999. User's guide to PHREEQC (version 2)–a computer program for speciation, batch-reaction, one-dimensional transport, and inverse geochemical calculations. Water-Resour. Invest Report 99, 312.
Pierrot, D., Millero, F.J., 2016. The speciation of metals in natural waters. Aquat. Geochem. 1–20.
Plummer, L.N., Busenberg, E., 1982. The solubilities of calcite, aragonite and vaterite in CO2-H2O solutions between 0 and 90 C, and an evaluation of the aqueous model for the system CaCO3-CO2-H2O. Geochem. Cosmochim. Acta 46, 1011–1040.
Pokrovsky, O., Mielczarski, J., Barres, O., Schott, J., 2000. Surface speciation models of calcite and dolomite/aqueous solution interfaces and their spectroscopic evaluation. Langmuir 16, 2677–2688.
Pokrovsky, O., Schott, J., 2002. Surface chemistry and dissolution kinetics of divalent metal carbonates. Environ. Sci. Technol. 36, 426–432.
Pokrovsky, O.S., Schott, J., 1999. Processes at the magnesium-bearing carbonates/solution interface. II. Kinetics and mechanism of magnesite dissolution. Geochem. Cosmochim. Acta 63, 881–897.
Pokrovsky, O.S., Schott, J., Thomas, F., 1999. Dolomite surface speciation and reactivity in aquatic systems. Geochem. Cosmochim. Acta 63, 3133–3143.
Prastka, K., Sanders, R., Jickells, T., 1998. Has the role of estuaries as sources or sinks of dissolved inorganic phosphorus changed over time? Results of a Kd study. Mar. Pollut. Bull. 36, 718–728.
Reddy, K., Graetz, D., 1981. Use of shallow reservoir and flooded organic soil systems for waste water treatment: nitrogen and phosphorus transformations. J. Environ. Qual. 10, 113–119.
Richardson, C.J., 1985. Mechanisms controlling phosphorus retention capacity in freshwater wetlands. Science 228, 1424–1427.
Riemersma, S., Little, J., Ontkean, G., Moskal-Hébert, T., 2006. Phosphorus Sources and Sinks in Watersheds: A Review, p. 82. Alberta soil phosphorus limits project 5.
Roden, E., Edmonds, J., 1997. Phosphate mobilization in iron-rich anaerobic sediments: microbial Fe (III) oxide reduction versus iron-sulfide formation. Arch. Hydrobiol. 139, 347–378.
Salimi, M., Heughebaert, J., Nancollas, G., 1985. Crystal growth of calcium phosphates in the presence of magnesium ions. Langmuir 1, 119–122.
Sekkal, W., Zaoui, A., 2013. Nanoscale analysis of the morphology and surface stability of calcium carbonate polymorphs. Sci. Rep. 3.
Shariatmadari, H., Mermut, A., 1999. Magnesium-and silicon-induced phosphate desorption in smectite–, palygorskite–, and sepiolite–calcite systems. Soil Sci. Soc. Am. J. 63, 1167–1173.
Shinn, E., 1973. Carbonate Coastal Accretion in an Area of Longshore Transport, NE Qatar, Persian Gulf. The Persian Gulf. Springer, pp. 179–191.
Sø, H.U., Postma, D., Jakobsen, R., Larsen, F., 2008. Sorption and desorption of arsenate and arsenite on calcite. Geochem. Cosmochim. Acta 72, 5871–5884.
Sø, H.U., Postma, D., Jakobsen, R., Larsen, F., 2011. Sorption of phosphate onto calcite; results from batch experiments and surface complexation modeling. Geochem. Cosmochim. Acta 75, 2911–2923.
Syers, J., Browman, M., Smillie, G., Corey, R., 1973. Phosphate sorption by soils evaluated by the Langmuir adsorption equation. Soil Sci. Soc. Am. J. 37, 358–363.
Van Cappellen, P., Charlet, L., Stumm, W., Wersin, P., 1993. A surface complexation model of the carbonate mineral-aqueous solution interface. Geochem. Cosmochim. Acta 57, 3505–3518.
Vitousek, P.M., Porder, S., Houlton, B.Z., Chadwick, O.A., 2010. Terrestrial phosphorus limitation: mechanisms, implications, and nitrogen–phosphorus interactions. Ecol. Appl. 20, 5–15.
Wang, S., Kong, L., Long, J., Su, M., Diao, Z., Chang, X., Chen, D., Song, G., Shih, K., 2018. Adsorption of phosphorus by calcium-flour biochar: isotherm, kinetic and transformation studies. Chemosphere 195, 666–672.
Wolthers, M., Di Tommaso, D., Du, Z., de Leeuw, N., 2012. Calcite surface structure and reactivity: molecular dynamics simulations and macroscopic surface modelling of the calcite–water interface. Phys. Chem. Chem. Phys. 14, 15145–15157.
Yadav, B., Paliwal, K., Nimgade, N., 1984. Effect of magnesium-rich waters on phosphate adsorption by calcite. Soil Sci. 138, 153–157.
Yakubu, M., Gumel, M., Abdullahi, A., 2008. Use of activated carbon from date seeds to treat textile and tannery effluents. African Journal of Science and Technology (AJST) Science and Engineering Series 9, 39–49.
Zak, D., Kleeberg, A., Hupfer, M., 2006. Sulphate-mediated phosphorus mobilization in riverine sediments at increasing sulphate concentration, River Spree, NE Germany. Biogeochemistry 80, 109–119.
Zhang, J.-Z., Huang, X.-L., 2011. Effect of temperature and salinity on phosphate sorption on marine sediments. Environ. Sci. Technol. 45, 6831–6837.
Zhang, P., Austad, T., 2006. Wettability and oil recovery from carbonates: effects of temperature and potential determining ions. Colloids Surf. A Physicochem. Eng. Asp. 279, 179–187.
Zhou, A., Tang, H., Wang, D., 2005. Phosphorus adsorption on natural sediments: modeling and effects of pH and sediment composition. Water Res. 39, 1245–1254.
Zhou, M., Li, Y., 2001. Phosphorus-sorption characteristics of calcareous soils and limestone from the southern Everglades and adjacent farmlands. Soil Sci. Soc. Am. J. 65, 1404–1412.